The Astrophysical Journal, 977:232 (5pp), 2024 December 20 https://doi.org/10.3847/1538-4357/ad932f

Fast Radio Bursts and Interstellar Objects

Dang Pham[1,5], Matthew J. Hopkins[2,5], Chris Lintott[2], Michele T. Bannister[3], and Hanno Rein[1,4]
[1] Department of Astronomy and Astrophysics, University of Toronto, Toronto, Ontario, M5S 3H4, Canada; dang.pham@astro.utoronto.ca
[2] Department of Physics, University of Oxford, Denys Wilkinson Building, Keble Road, Oxford, OX1 3RH, UK; matthew.hopkins@physics.ox.ac.uk
[3] School of Physical and Chemical Sciences—Te Kura Matū, University of Canterbury, Private Bag 4800, Christchurch 8140, New Zealand
[4] Department of Physical and Environmental Sciences, University of Toronto at Scarborough, Toronto, Ontario M1C 1A4, Canada
Received 2024 September 27; revised 2024 November 4; accepted 2024 November 8; published 2024 December 17

Abstract

Fast radio bursts (FRBs) are transient radio events with millisecond-scale durations and debated origins. Collisions between planetesimals and neutron stars (NSs) have been proposed as a mechanism to produce FRBs; the planetesimal strength, size, and density determine the time duration and energy of the resulting event. One source of planetesimals is the population of interstellar objects (ISOs), free-floating objects expected to be extremely abundant in galaxies across the Universe as products of planetary formation. We explore using the ISO population as a reservoir of planetesimals for FRB production, finding that the expected ISO–NS collision rate is comparable with the observed FRB event rate. Using a model linking the properties of planetesimals and the FRBs they produce, we further show that observed FRB durations are consistent with the sizes of known ISOs, and the FRB energy distribution is consistent with the observed size distributions of solar system planetesimal populations. Finally, we argue that the rate of ISO–NS collisions must increase with cosmic time, matching the observed evolution of the FRB rate. Thus, ISO–NS collisions are a feasible mechanism for producing FRBs.

Unified Astronomy Thesaurus concepts: Radio bursts (1339); Interstellar objects (52); Asteroids (72); Neutron stars (1108)

1. Introduction

Fast radio bursts (FRBs) are gigahertz radio-emitting, millisecond-timescale transient events. First detected in 2007 (D. R. Lorimer et al. 2007), a large catalog has been assembled by the Canadian Hydrogen Intensity Mapping Experiment (CHIME; CHIME/FRB Collaboration et al. 2021). The majority of known FRBs are extragalactic (A. G. Mannings et al. 2021), with only one yet known in the Milky Way (C. D. Bochenek et al. 2020; CHIME/FRB Collaboration et al. 2020). They exist in a wide range of host galaxies and local environments, but remain sparse: the inferred volumetric FRB rate for events above a threshold energy of 10^{35} erg is $(7^{+9}_{-6}) \times 10^{7}$ Gpc^{-3} yr^{-1} (C. D. Bochenek et al. 2020). Two types are known: single (one-off) events, and repeating FRBs.

One of the many (see E. Platts et al. 2019; B. Zhang 2020) proposed mechanisms to produce an FRB is a collision between a planetesimal and a neutron star (NS), initially suggested by J. J. Geng & Y. F. Huang (2015). Though NSs have been found to have planetary systems bound to them (A. Wolszczan & D. A. Frail 1992), the radiation mechanism of J. J. Geng & Y. F. Huang (2015) is specifically for unbound planetesimals, colliding on radial trajectories, as bound planetesimals are expected to interact differently (P. R. Brook et al. 2014). Z. G. Dai et al. (2016) and M. Bagchi (2017) invoked the mechanism of J. J. Geng & Y. F. Huang (2015) to explain repeating FRBs as NSs undergoing frequent encounters in debris disks around other stars. However, the feasibility of this scenario producing repeating FRBs at the rate observed is debated (J. L. Smallwood et al. 2019; C. Deng et al. 2024). Nevertheless, nonrepeating FRBs may still be generated by NS–planetesimal collisions, if impacts can occur at a suitable rate in free space.

In this work, we consider the collisions between NS and interstellar objects (ISOs). An expected feature of planet formation (T. A. McGlynn & R. D. Chapman 1989), ISOs are planetesimals unbound from the planetary systems they formed in 'Oumuamua ISSI Team et al. (2019) with a density of 10^{15} pc^{-3} in the solar neighborhood (A. Do et al. 2018) and a total number of $\sim 10^{27}$ across the Milky Way, and two discovered so far: 1I/'Oumuamua and 2I/Borisov. We first quantify the ISO–NS collision rate and consider its implications (Section 2). We then use the radiation mechanism of Z. G. Dai et al. (2016) to compare the observed durations and energetics of FRBs to the sizes of ISOs (Section 3). Finally, in Section 4, we discuss testable implications of FRBs being produced by ISO–NS collisions, and challenges with scaling the ISO–NS collision rate with the FRB event rate.

2. ISO–NS Collision Rate

In this section, we first detail our estimate for the ISO–NS collision rate, and then discuss sources of uncertainty in our estimate.

To estimate the density and velocity distribution of ISOs around NSs we make a number of assumptions. Since ISOs are an abundant, expected product of planetary systems (E. M. Shoemaker & R. F. Wolfe 1984; S. A. Stern 1990; D. Jewitt & D. Z. Seligman 2023), we first assume that planetary systems, and therefore ISO populations, are present in galaxies throughout the Universe. The population of ISOs larger than 1I/'Oumuamua passing through the solar system has a number density of $n_{\rm ISO} \sim 10^{15}$ pc^{-3} (A. Do et al. 2018), and a velocity distribution with a width of approximately 50 km s^{-1} (M. J. Hopkins et al. 2024). Being estimated from a single

[5] DP and MJH contributed equally.

detection in a well-characterized survey, this estimated number density has an uncertainty of 1 order of magnitude, but lacking additional constraints, we assume the number density of ISOs around all NSs will be the same order of magnitude as this. For the relative velocities of NS and ISOs, we note that upon creation, NSs receive a large natal kick on the order of $\sim 100\,\mathrm{km\,s^{-1}}$ (A. G. Lyne & D. R. Lorimer 1994; G. Hobbs et al. 2005). As this is significantly larger than the ISO velocity dispersion around the Sun, we assume this value for the relative speed v_∞ of ISOs encountering NSs.

In the vicinity of an NS of mass $M_{\rm NS} \simeq 1.4\,M_\odot$ (A. Heger et al. 2003), ISOs follow hyperbolic trajectories defined by their impact parameter b and relative speed at infinity v_∞, related to the periastron q by $b^2 = q^2\left(1 + \frac{2GM_{\rm NS}}{qv_\infty^2}\right)$. An ISO impacts the NS surface when it has a periastron less than the NS radius $R_{\rm NS} \simeq 10\,\mathrm{km}$ (M. C. Miller et al. 2021); therefore, the cross section of ISOs with a relative speed at infinity v_∞ colliding with the NS surface is

$$\sigma = \pi b^2 = \pi R_{\rm NS}^2\left(1 + \frac{2GM_{\rm NS}}{v_\infty^2 R_{\rm NS}}\right) \approx 10^9\,\mathrm{km}^2\left(\frac{M_{\rm NS}}{1.4\,M_\odot}\right)\left(\frac{R_{\rm NS}}{10\,\mathrm{km}}\right)\left(\frac{v_\infty}{100\,\mathrm{km\,s^{-1}}}\right)^{-2}. \quad (1)$$

The increase in cross section due to the second term is referred to as gravitational focusing (see J. C. Forbes & A. Loeb 2019) and completely dominates in this high-gravity situation. Thus, taking $n_{\rm ISO} \sim 10^{15}\,\mathrm{pc^{-3}}$, $v_\infty \sim 100\,\mathrm{km\,s^{-1}}$, and $\sigma \sim 10^9\,\mathrm{km}^2$ gives the encounter rate of a single NS with ISOs as

$$\Gamma = n_{\rm ISO} v_\infty \sigma \sim 10^{-7}\,\mathrm{yr^{-1}}. \quad (2)$$

FRBs are detected over cosmological distances, with the most distant being detected at $z = 1$ (S. D. Ryder et al. 2023); thus, we must consider the cosmological rate of ISO–NS collisions. Stars over $9M_\odot$ make up $\sim$0.5% of all stars formed (assuming the Universal initial mass function of P. Kroupa 2001), have lifetimes $\lesssim$0.1 Gyr, and largely form NSs upon their deaths (A. Heger et al. 2003). Thus, with approximately 10^{11} stars (e.g., T. C. Licquia & J. A. Newman 2015), the Milky Way contains about $N_{\rm NS} \sim 10^9$ NS. For a number density of Milky Way-mass galaxies of $n_{\rm Gal} \sim 10^7\,\mathrm{Gpc^{-3}}$ (M. R. Blanton et al. 2003), the cosmological rate of ISO–NS collisions is

$$R_{\rm col} = \Gamma \cdot n_{\rm Gal} \cdot N_{\rm NS} \sim 10^9\,\mathrm{Gpc^{-3}\,yr^{-1}}. \quad (3)$$

FRBs produced by ISO–NS collisions are thought to be strongly beamed by a factor $f \sim 10^{-2}$ (Z. G. Dai 2020), meaning if every 1I-sized ISO–NS collision produced an FRB the observable rate would be

$$R_{\rm obs} = fR_{\rm col} \sim 10^7\,\mathrm{Gpc^{-3}\,yr^{-1}}, \quad (4)$$

comparable to the observed rate of $(7^{+9}_{-6}) \times 10^7\,\mathrm{Gpc^{-3}\,yr^{-1}}$ (C. D. Bochenek et al. 2020).

The most significant source of uncertainty in this estimate is the average number density of ISOs $n_{\rm ISO}$ around NSs. In addition to the order-of-magnitude uncertainty in the number density of ISOs in the solar neighborhood, ISOs are not directly observable outside the solar system, so the density around different NSs across the local Universe may vary significantly from this value. We expect the density of ISOs to vary across the Milky Way (M. J. Hopkins et al. 2023) and between different galaxies (T. G. Williams et al. 2022) due to a dependence of planetesimal formation on stellar metallicity (G. Andama et al. 2024). Second, the natal kick that an NS receives (S. Chatterjee et al. 2005; G. Hobbs et al. 2005) can place them on an orbit removed from their galaxy's stars and ISOs, or completely eject them. D. Sweeney et al. (2022) model the Milky Way, predicting that 40% of NSs are completely ejected and the remaining NSs occupy a disk with a vertical scale height 5 times that of the stellar disk. ISOs are expected to retain the same spatial distribution as their parent stars (M. J. Hopkins et al. 2024); therefore, NS natal kicks could reduce the expected ISO–NS collision rate. This, however, will not be a major effect in elliptical galaxies, which make up $\sim$40% of galaxies in the local Universe brighter than $M_r < -19$ (C. J. Lintott et al. 2008; M_r is the r-band absolute magnitude).

Finally, the timescale for a typical collision between an ISO and an NS (Equation (2)) is far longer than that of repeating FRBs, which occur on a timescale of weeks. Thus, we find that ISO–NS collisions cannot explain repeating FRBs and this mechanism cannot be the only source of FRBs.[6] However, we can make testable predictions from the potential subset of FRBs caused by ISO–NS collisions.

3. Emission Properties

We now explore the expected properties assuming the emission mechanism predicted in J. J. Geng & Y. F. Huang (2015), Z. G. Dai et al. (2016), and Z. G. Dai (2020). When the tidal forces on the planetesimal exceed its tensile strength s, it will be disrupted. This has been observed in the solar system, for example in the tidal disruption of comet Shoemaker–Levy 9 (SL9) by Jupiter (A. P. Boss 1994). Small bodies in the solar system—like asteroids and comets—are rubble piles (e.g., E. Asphaug & W. Benz 1994; K. J. Walsh 2018) with a low tensile strength. S. A. Colgate & A. G. Petschek (1981) use a tensile strength $s \sim 10^9$ Pa and this value is continued in later works (such as J. J. Geng & Y. F. Huang 2015; Z. G. Dai et al. 2016; A. Siraj & A. Loeb 2019). However, asteroids and comets have significantly lower values, $s \sim 500$ Pa (as constrained by spacecraft measurement and population analysis; e.g., J. M. Greenberg et al. 1995; N. Attree et al. 2018; D. J. Scheeres 2018). Likewise, the compressive strength, $P_0 \sim 100$ MPa (e.g., P. Jenniskens et al. 2012; G. J. Flynn et al. 2018; L. Pohl & D. T. Britt 2020), is 3 orders of magnitude lower than in S. A. Colgate & A. G. Petschek (1981). We use these current estimates of tensile and compressive strengths in the context of the Z. G. Dai et al. (2016) emission mechanism.

An ISO–NS collision produces homogeneous tidal disruption, in contrast to an SL9-like disruption. On a highly elliptical orbit around Jupiter, SL9 passed close enough to the planet at perijove to partially disrupt into several fragments in 1992 (S. Nakano et al. 1993). However, it then continued on its orbit, far enough from Jupiter that no more disruption events occurred, for an additional 2 yr before colliding with the planet in 1994 (D. H. Levy 1998), allowing the fragments to drift a significant distance apart. In an ISO–NS collision as modeled in S. A. Colgate & A. G. Petschek (1981), J. J. Geng & Y. F. Huang (2015), and Z. G. Dai et al. (2016), the

[6] The contribution of multiple different mechanisms to the FRB population has been suggested in, e.g., A. C. Gordon et al. (2023). Furthermore, Z. Pleunis et al. (2021) find differences in the emissions from repeaters and nonrepeaters, implying repeaters and nonrepeaters have different progenitors.

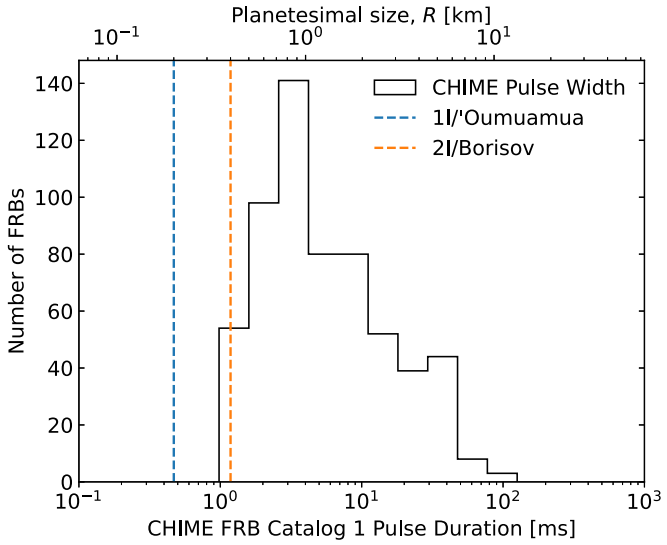

Figure 1. The CHIME Catalog 1 distribution of FRB boxcar pulse width. On the top axis, we show the equivalent planetesimal size, R, assuming tensile strength $s = 500$ Pa and density $\rho_0 = 3$ g cm^{-3}. Dashed vertical lines show the estimated sizes of two observed ISOs, 1I/'Oumuamua and 2I/Borisov. The apparent sudden cutoff in FRB pulse duration at 10^0 ms is due to CHIME's time resolution (0.983 ms; CHIME/FRB Collaboration et al. 2021).

planetesimal falls radially onto the NS, impacting the surface very shortly after fragmentation begins. As it approaches the NS and the tidal forces on it continually increase, the planetesimal will go through a rapid sequence of disruptions, with each generation of fragments undergoing their own fragmentation each time the remaining distance to the NS decreases by a factor of $2^{-2/9} \simeq 0.85$ (S. A. Colgate & A. G. Petschek 1981). Thus, the planetesimal will completely disrupt into a mostly homogeneous stream of material, and we expect ISO–NS collisions to produce largely unstructured FRBs, without subbursts.[7]

After disruption, the time difference between the arrival of the leading and trailing edge of the disrupted planetesimal fragments is given by S. A. Colgate & A. G. Petschek (1981), with ρ and R as the density and radius of the planetesimal:

$$\Delta t \simeq 4\ \mathrm{ms}\left(\frac{M_{\rm NS}}{1.4M_\odot}\right)^{-1/3}\left(\frac{\rho}{3\ \mathrm{g\ cm^{-3}}}\right)^{1/6} \cdot \left(\frac{s}{500\ \mathrm{Pa}}\right)^{-1/6}\left(\frac{R}{1\ \mathrm{km}}\right)^{4/3}. \quad (5)$$

This relates planetesimal radius to the resulting FRB duration. In Figure 1, we show the histogram of FRBs' duration from CHIME Catalog 1 (CHIME/FRB Collaboration et al. 2021) with equivalent planetesimal radii, R. Note that there is an apparent cutoff in FRB pulse duration at $\sim$1 ms due to CHIME's time resolution (CHIME/FRB Collaboration et al. 2021). The distribution plotted here is subject to detection bias: as discussed later, the longer FRB pulses produced by larger ISOs are also brighter, and therefore more detectable. Though a full model of the detection bias present in CHIME is beyond the scope of this work, we can qualitatively say that the distribution plotted in Figure 1 will be weighted toward longer pulse lengths and larger ISO radii than the underlying distribution. However, the observed range of FRB durations corresponds to planetesimal radii $400\ \mathrm{m} \lesssim R \lesssim 10\ \mathrm{km}$, still broadly consistent with the sizes of the two observed ISOs (D. Jewitt et al. 2017; M.-T. Hui et al. 2020).

Using the updated value for tensile strength we can reinterpret the potential asteroidal cause of FRB 200428, first postulated in Z. G. Dai (2020). FRB 200428 consists of two distinct subbursts of 0.6 and 0.3 ms separated by a large gap of 29 ms (see Figure 1 of CHIME/FRB Collaboration et al. 2020). Assuming FRB 200428 was caused by an ISO–NS collision, Z. G. Dai (2020) suggests that these subbursts were caused by two major fragments of a single body, split through tidal disruption during infall. As discussed earlier in this section, we expect instead that tidal disruption during infall onto an NS will not create two major fragments but instead a mostly homogeneous stream of material. Thus, we tentatively suggest instead that the large and complete separation of the subbursts is evidence that the colliding ISO was a binary: two separate bodies of radius 200 and 100 m, respectively, with a separation of several kilometers. Binaries are common within the solar system (J. L. Margot et al. 2002; K. J. Walsh et al. 2008; W. C. Fraser et al. 2017), but the potential existence of binary ISOs presents a fascinating opportunity for study. If formed as a binary before ejection from their home planetary systems, the ejection mechanism must be gentle enough to allow the constituent bodies to remain gravitationally bound. C. H. McDonald & D. Veras (2023) find that ejection by scattering off planets disrupts all binary asteroids; however, ejection mechanisms acting at larger stellocentric distances, such as stellar flybys (S. Pfalzner et al. 2021) or the effect of the Galactic tide on the outer edges of exo-Oort clouds (R. Brasser et al. 2010; N. A. Kaib et al. 2011) may be sufficiently gentle. Alternatively, binaries could perhaps be formed in the tidal disruption events that may be the source of some ISOs (K. J. Walsh & D. C. Richardson 2006; M. Ćuk 2018; Y. Zhang & D. N. C. Lin 2020). An interesting prediction of connecting FRB subbursts to binary ISOs is that they should be largely limited to two subbursts, since triple (and higher) asteroids are much rarer. We find that of the nonrepeating FRBs in the CHIME Catalog 1, there are 450 events consisting of 1 burst, 19 events with 2 subbursts, and only 5 events with more than 2 subbursts. As discussed above, ISO–NS collisions cannot be the source of all FRBs, but if they are the source of some, then FRBs may potentially be a probe for studying ISOs well beyond the limits of the solar system.

Now we relate the luminosity distribution of FRBs to possible size distributions of ISOs. Under the Z. G. Dai et al. (2016) mechanism, most of the energy is released at frequency $\sim$1 GHz, consistent with the FRBs energy spectrum. The luminosity is given by

$$L_{\rm tot} \sim 2.5 \times 10^{36}\ \mathrm{erg\ s^{-1}}\left(\frac{P_0}{100\ \mathrm{MPa}}\right)^{2/5}\left(\frac{s}{500\ \mathrm{Pa}}\right)^{4/15} \cdot \left(\frac{R}{1\ \mathrm{km}}\right)^{8/3}\left(\frac{\rho}{3\ \mathrm{g\ cm^{-3}}}\right)^{-2/3}\left(\frac{M_{\rm NS}}{1.4\ M_\odot}\right)^{19/12} \cdot \left(\frac{\mu_B}{10^{30}\ \mathrm{G\ cm^3}}\right)^{3/2}\left(\frac{d}{10\ \mathrm{km}}\right)^{-23/4}\left(\frac{\rho_c}{10^6\ \mathrm{cm}}\right)^{-1}, \quad (6)$$

[7] This is the case even for contact binaries such as (486958) Arrokoth or 67P/Churyumov–Gerasimenko, made up of two distinct lobes held together by mutual gravity (D. J. Scheeres 2007), as the tidal force required to separate two lobes is the same order of magnitude as that required to disrupt each lobe individually.

Table 1
Planetesimal Size Distributions, Power-law Exponents q, and the Resultant Predicted ISO–NS Collision Energy Distribution Exponent γ Compared to the Observed FRB Energy Distribution Exponent

q	γ	Description
2.5	1.38	Main asteroid belt (B. J. Gladman et al. 2009)
2.8	1.45	Streaming instability (J. B. Simon et al. 2016)
3.5	1.63	Faint trans-Neptunian objects (TNOs; S. M. Lawler et al. 2018)
...	$1.3^{+0.7}_{-0.4}$	Observed FRBs (K. Shin et al. 2023)

where $\mu_B = B_{\rm surface} R_{\rm NS}^3$ is the magnetic dipole moment, $B_{\rm surface}$ is the field strength at the NS surface, ρ_c is the curvature radius near the NS, and d is the distance from the ionized planetesimal fragments to the NS center. The strong dependence on d implies that most of the energy is released near the NS surface at $d \simeq R_{\rm NS} \simeq 10$ km. This emission is strongly beamed by a factor $f \sim 1/100$, so the isotropic-equivalent energy emission is given by $E_{\rm isotropic} \sim L_{\rm tot}\Delta t/f$. Observed FRBs have isotropic energy emission typically between 10^{35} and 10^{41} erg (CHIME/FRB Collaboration et al. 2020; F. Kirsten et al. 2024), equivalent to planetesimal sizes $0.5-10$ km at typical pulsar magnetic field strengths, consistent with sizes inferred from FRB time duration.

The observed isotropic energy distribution of FRBs appears to follow a power law:

$$\frac{dN}{dE_{\rm isotropic}} \propto E_{\rm isotropic}^{-\gamma}, \tag{7}$$

with γ inferred to be $1.3^{+0.7}_{-0.4}$ by K. Shin et al. (2023). Planetesimal size distributions are typically also treated as power laws or composite power laws:

$$\frac{dN}{dR} \propto R^{-q}, \tag{8}$$

with streaming instability modeling predicting $q \approx 2.8$ (J. B. Simon et al. 2016), and observations of solar system populations finding values of $q \approx 2.5$ for the main asteroid belt (B. J. Gladman et al. 2009) and $q \approx 3.5$ for faint trans-Neptunian objects (e.g., S. M. Lawler et al. 2018). The ISO size distribution is completely unconstrained, but assuming ISOs have a similar power-law size distributions to solar system populations, we can relate the ISO power-law exponent to the expected ISO–NS isotropic energy distribution exponent. Since $E_{\rm isotropic} \propto L_{\rm tot}\Delta t \propto R^4$, γ is related to q by $\gamma = (3+q)/4$.

Table 1 compares the expected values of γ for ISO–NS collision isotropic energy distributions assuming different planetesimal size distributions to the observed FRB distribution. Ideally, we would compare our predictions for γ to the energy distribution of exclusively single pulses from nonrepeating FRBs, as this is the type of FRB that our model predicts. However, the sample used by K. Shin et al. (2023) includes repeating FRBs, albeit only the first detected burst from each and uses the combined energy released in the small number of FRBs with multiple pulses. Since the majority of bursts are single pulses from nonrepeaters, we do not expect this to change the value of γ by a significant amount and find that the power-law scalings are within the uncertainty of observed FRB rates.

4. Discussion

First, both NSs and ISOs are long-lived and build up over time, meaning that the rate of ISO–NS collisions is decoupled from the current star formation rate. This is in direct contrast to magnetars, a commonly invoked FRB source (e.g., B. Margalit et al. 2019; B. D. Metzger et al. 2019; Z. Wadiasingh & A. Timokhin 2019), which have short lifetimes of 10 kyr (T. Mondal 2021), meaning they are only present when and where star-forming is actively occurring. Several recent studies have found the redshift dependence of the FRB rate to be inconsistent with the evolution of the cosmic star formation rate (e.g., T. Hashimoto et al. 2020a, 2022; R. C. Zhang & B. Zhang 2022; L. Tang et al. 2023; J. H. Chen et al. 2024; H.-N. Lin & R. Zou 2024; H.-N. Lin et al. 2024; K. J. Zhang et al. 2024), and FRBs cannot only originate from short-lived objects like magnetars. Instead of decreasing with cosmic time like the star formation rate (P. Madau & M. Dickinson 2014), the FRB rate is increasing, as would be expected from long-lived progenitors.

Second, a small number of FRBs have been localized to their host galaxies, and though the majority of this sample is found in star-forming galaxies, those that originate in quiescent galaxies are unlikely to be from young progenitors (A. C. Gordon et al. 2023). If ISO–NS collisions are the source of a significant fraction of FRBs, we additionally would expect the reduced rate of ISO–NS collisions from disk galaxies as NS natal kicks cause a dependence of FRB rate on host galaxy morphology.

Therefore, we expect that insights into ISO–NS as a production mechanism will be constrained as more events are found and localized by Square Kilometre Array, CHIME, CHORD, and ASKAP (K. Vanderlinde et al. 2019; S. Bhandari et al. 2020; T. Hashimoto et al. 2020b; D. Michilli et al. 2023).

A final issue remains: the rate of observable ISO–NS collisions of $\sim 10^7\,{\rm Gpc^{-3}\,yr^{-1}}$ that we calculate in Section 2 is not directly comparable to the rate of FRBs of $(7^{+9}_{-6}) \times 10^7\,{\rm Gpc^{-3}\,yr^{-1}}$ inferred by C. D. Bochenek et al. (2020). The rate we calculate corresponds to 1I-sized ISOs colliding with all NSs, whereas the observable FRB rate inferred by C. D. Bochenek et al. (2020) corresponds to FRBs of at least the energy of FRB 200428, with an isotropic-equivalent energy release of 2×10^{35} erg. Ideally, we would use a combination of the ISO size distribution and NS magnetic field distribution to calculate the rate distribution of ISO–NS collision energies, and compare the observable ISO–NS collision rate at the energy of FRB 200428. However, given that the ISO size distribution is not well-constrained, this is beyond the scope of this work.

5. Conclusion

The progenitors and emission mechanisms of FRBs are debated. We revisit the emission mechanism of J. J. Geng & Y. F. Huang (2015) and Z. G. Dai et al. (2016), which postulate FRBs are caused by collisions between NSs and planetesimals, and investigate the implications of these planetesimals being ISOs. As products of planetary formation, ISOs are common in the Milky Way and expected to be abundant across the Universe. We have demonstrated that the expected ISO–NS

collision rate is consistent with the cosmic rate of FRBs within the order-of-magnitude uncertainties. Using updated planetesimal properties, such as tensile strength, we have shown that observed FRB durations and energetics correspond to collisions with planetesimals of sizes in the range 0.4−10 km, consistent with the two observed ISOs. We have tentatively suggested FRBs with subbursts such as FRB 200428 could be caused by collisions with binary ISOs. Finally, we have discussed the testable implications of ISO–NS collisions producing FRB-like signals on the redshift dependence of the FRB rate, and the morphology of galaxies that host FRBs. Thus, collisions between ISOs and NSs are feasible progenitors of one-off FRBs.

Acknowledgments

We thank the anonymous reviewer for the insightful comments. We would like to thank Jocelyn Bell Burnell, Ayush Pandhi, and Alexander Andersson for insightful and helpful discussions. M.J.H. acknowledges support from the Science and Technology Facilities Council through grant ST/W507726/1.

ORCID iDs

Dang Pham https://orcid.org/0000-0002-0924-8403
Matthew J. Hopkins https://orcid.org/0000-0001-6314-873X
Chris Lintott https://orcid.org/0000-0001-5578-359X
Michele T. Bannister https://orcid.org/0000-0003-3257-4490
Hanno Rein https://orcid.org/0000-0003-1927-731X

References

Andama, G., Mah, J., & Bitsch, B. 2024, A&A, 683, A118
Asphaug, E., & Benz, W. 1994, Natur, 370, 120
Attree, N., Groussin, O., Jorda, L., et al. 2018, A&A, 611, A33
Bagchi, M. 2017, ApJL, 838, L16
Bhandari, S., Sadler, E. M., Prochaska, J. X., et al. 2020, ApJL, 895, L37
Blanton, M. R., Hogg, D. W., Bahcall, N. A., et al. 2003, ApJ, 592, 819
Bochenek, C. D., Ravi, V., Belov, K. V., et al. 2020, Natur, 587, 59
Boss, A. P. 1994, Icar, 107, 422
Brasser, R., Higuchi, A., & Kaib, N. 2010, A&A, 516, A72
Brook, P. R., Karastergiou, A., Buchner, S., et al. 2014, ApJL, 780, L31
Chatterjee, S., Vlemmings, W. H. T., Brisken, W. F., et al. 2005, ApJL, 630, L61
Chen, J. H., Jia, X. D., Dong, X. F., & Wang, F. Y. 2024, ApJL, 973, L54
CHIME/FRB Collaboration, Amiri, M., Andersen, B. C., et al. 2021, ApJS, 257, 59
CHIME/FRB Collaboration, Andersen, B. C., Bandura, K. M., et al. 2020, Natur, 587, 54
Colgate, S. A., & Petschek, A. G. 1981, ApJ, 248, 771
Ćuk, M. 2018, ApJL, 852, L15
Dai, Z. G. 2020, ApJL, 897, L40
Dai, Z. G., Wang, J. S., Wu, X. F., & Huang, Y. F. 2016, ApJ, 829, 27
Deng, C., Huang, Y.-F., Du, C., Wang, P., & Dai, Z.-G. 2024, ApJ, 974, 215
Do, A., Tucker, M. A., & Tonry, J. 2018, ApJL, 855, L10
Flynn, G. J., Consolmagno, G. J., Brown, P., & Macke, R. J. 2018, ChEG, 78, 269
Forbes, J. C., & Loeb, A. 2019, ApJL, 875, L23
Fraser, W. C., Bannister, M. T., Pike, R. E., et al. 2017, NatAs, 1, 0088
Geng, J. J., & Huang, Y. F. 2015, ApJ, 809, 24
Gladman, B. J., Davis, D. R., Neese, C., et al. 2009, Icar, 202, 104
Gordon, A. C., Fong, W.-f., Kilpatrick, C. D., et al. 2023, ApJ, 954, 80
Greenberg, J. M., Mizutani, H., & Yamamoto, T. 1995, A&A, 295, L35
Hashimoto, T., Goto, T., Chen, B. H., et al. 2022, MNRAS, 511, 1961
Hashimoto, T., Goto, T., On, A. Y. L., et al. 2020a, MNRAS, 498, 3927
Hashimoto, T., Goto, T., On, A. Y. L., et al. 2020b, MNRAS, 497, 4107
Heger, A., Fryer, C. L., Woosley, S. E., Langer, N., & Hartmann, D. H. 2003, ApJ, 591, 288
Hobbs, G., Lorimer, D. R., Lyne, A. G., & Kramer, M. 2005, MNRAS, 360, 974
Hopkins, M. J., Bannister, M. T., & Lintott, C. 2024, arXiv:2402.04904
Hopkins, M. J., Lintott, C., Bannister, M. T., Mackereth, J. T., & Forbes, J. C. 2023, AJ, 166, 241
Hui, M.-T., Ye, Q.-Z., Föhring, D., Hung, D., & Tholen, D. J. 2020, AJ, 160, 92
Jenniskens, P., Fries, M. D., Yin, Q.-Z., et al. 2012, Sci, 338, 1583
Jewitt, D., Luu, J., Rajagopal, J., et al. 2017, ApJL, 850, L36
Jewitt, D., & Seligman, D. Z. 2023, ARA&A, 61, 197
Kaib, N. A., Roškar, R., & Quinn, T. 2011, Icar, 215, 491
Kirsten, F., Ould-Boukattine, O. S., Herrmann, W., et al. 2024, NatAs, 8, 337
Kroupa, P. 2001, MNRAS, 322, 231
Lawler, S. M., Shankman, C., Kavelaars, J. J., et al. 2018, AJ, 155, 197
Levy, D. H. 1998, SSRv, 85, 523
Licquia, T. C., & Newman, J. A. 2015, ApJ, 806, 96
Lin, H.-N., Li, X.-Y., & Zou, R. 2024, ApJ, 969, 123
Lin, H.-N., & Zou, R. 2024, ApJ, 962, 73
Lintott, C. J., Schawinski, K., Slosar, A., et al. 2008, MNRAS, 389, 1179
Lorimer, D. R., Bailes, M., McLaughlin, M. A., Narkevic, D. J., & Crawford, F. 2007, Sci, 318, 777
Lyne, A. G., & Lorimer, D. R. 1994, Natur, 369, 127
Madau, P., & Dickinson, M. 2014, ARA&A, 52, 415
Mannings, A. G., Fong, W.-f., Simha, S., et al. 2021, ApJ, 917, 75
Margalit, B., Berger, E., & Metzger, B. D. 2019, ApJ, 886, 110
Margot, J. L., Nolan, M. C., Benner, L. A. M., et al. 2002, Sci, 296, 1445
McDonald, C. H., & Veras, D. 2023, MNRAS, 520, 4009
McGlynn, T. A., & Chapman, R. D. 1989, ApJL, 346, L105
Metzger, B. D., Margalit, B., & Sironi, L. 2019, MNRAS, 485, 4091
Michilli, D., Bhardwaj, M., Brar, C., et al. 2023, ApJ, 950, 134
Miller, M. C., Lamb, F. K., Dittmann, A. J., et al. 2021, ApJL, 918, L28
Mondal, T. 2021, ApJL, 913, L12
Nakano, S., Kobayashi, T., Meyer, E., et al. 1993, IAUC, 5800, 1
'Oumuamua ISSI Team, Bannister, M. T., Bhandare, A., et al. 2019, NatAs, 3, 594
Pfalzner, S., Aizpuru Vargas, L. L., Bhandare, A., & Veras, D. 2021, A&A, 651, A38
Platts, E., Weltman, A., Walters, A., et al. 2019, PhR, 821, 1
Pleunis, Z., Good, D. C., Kaspi, V. M., et al. 2021, ApJ, 923, 1
Pohl, L., & Britt, D. T. 2020, M&PS, 55, 962
Ryder, S. D., Bannister, K. W., Bhandari, S., et al. 2023, Sci, 382, 294
Scheeres, D. J. 2007, Icar, 189, 370
Scheeres, D. J. 2018, Icar, 304, 183
Shin, K., Masui, K. W., Bhardwaj, M., et al. 2023, ApJ, 944, 105
Shoemaker, E. M., & Wolfe, R. F. 1984, LPSC, 15, 780
Simon, J. B., Armitage, P. J., Li, R., & Youdin, A. N. 2016, ApJ, 822, 55
Siraj, A., & Loeb, A. 2019, RNAAS, 3, 130
Smallwood, J. L., Martin, R. G., & Zhang, B. 2019, MNRAS, 485, 1367
Stern, S. A. 1990, PASP, 102, 793
Sweeney, D., Tuthill, P., Sharma, S., & Hirai, R. 2022, MNRAS, 516, 4971
Tang, L., Lin, H.-N., & Li, X. 2023, ChPhC, 47, 085105
Vanderlinde, K., Liu, A., Gaensler, B., et al. 2019, Canadian Long Range Plan for Astronomy and Astrophysics White Papers, LRP2020 W028, Canadian Astronomical Society, 28
Wadiasingh, Z., & Timokhin, A. 2019, ApJ, 879, 4
Walsh, K. J. 2018, ARA&A, 56, 593
Walsh, K. J., & Richardson, D. C. 2006, Icar, 180, 201
Walsh, K. J., Richardson, D. C., & Michel, P. 2008, Natur, 454, 188
Williams, T. G., Kreckel, K., Belfiore, F., et al. 2022, MNRAS, 509, 1303
Wolszczan, A., & Frail, D. A. 1992, Natur, 355, 145
Zhang, B. 2020, Natur, 587, 45
Zhang, K. J., Dong, X. F., Rodin, A. E., et al. 2024, arXiv:2406.00476
Zhang, R. C., & Zhang, B. 2022, ApJL, 924, L14
Zhang, Y., & Lin, D. N. C. 2020, NatAs, 4, 852